J Therm Anal Calorim (2013) 111:2019–2028
DOI 10.1007/s10973-012-2247-0

Thermal behavior of some antihistamines

G. L. Perpétuo · D. A. Gálico · R. A. Fugita · R. A. E. Castro · M. E. S. Eusébio · O. Treu-Filho · A. C. M. Silva · G. Bannach

Received: 14 November 2011 / Accepted: 18 January 2012 / Published online: 4 February 2012

Abstract Thermogravimetry (TG), differential scanning calorimetry (DSC), polarized light thermal microscopy (PLTM), as well as X-ray powder diffraction (XRD) and Fourier transformed infrared spectroscopy (FTIR) were used to study the thermal behavior and the chemical structure of cimetidine, famotidine, ranitidine-HCl, and nizatidine. The TG–DSC curves show that the famotidine and ranitidine-HCl suffer decomposition during melting and they are thermally less stable in comparison with cimetidine and nizatidine, the latter being the most stable of all the drugs studied in this study. The DSC curves of famotidine and ranitidine-HCl show exothermic peaks immediately after the melting, confirming the occurrence of thermal decomposition. The DSC curves also show that the cimetidine and nizatidine have some thermal stability after melting. The thermal events shown in the PLTM images are consistent with the results shown in the TG–DSC and DSC curves. The XRD patterns show that the cimetidine and famotidine are less crystalline compared with ranitidine-HCl and nizatidine. The theoretical FTIR bands are in agreement with those obtained experimentally, and in some cases, no difference is observed between the theoretical and experimental values, even being identical in one of the cases.

Keywords Antihistamines · Thermal behavior · Cimetidine · Famotidine · Ranitidine · Nizatidine

Introduction

Cimetidine, famotidine, ranitidine, and nizatidine are drugs used for the ulcer treatment. They are histamine H2-receptor antagonists which are drugs capable of reducing the acid gastric secretion stimulated by histamine [1–4].

A pharmaceutical preparation consists of a drug(s) or active ingredient(s) together with so-called excipients or inactive ingredients (fillers, additives, etc.), all of which must be present in the correct proportions. Pharmaceutical preparations [5–8] provide the means by which pharmaceutically active substances or drugs can be supplied to the body, so that both the physiological considerations concerning the means of application (oral, cutaneous, subcutaneous, and rectal, etc.) and the physicochemical properties of the drug are suitable.

Thermal methods of analysis are widely used for checking thermal decomposition, thermal stability, polymorphism, reactions in solid state, drug formulations, purity, and other properties of solid compounds used in pharmaceutical industry [6–14]. Because of the numerous issues involved, it becomes important to have a complete understanding of the properties of pharmaceuticals.

G. L. Perpétuo · D. A. Gálico · R. A. Fugita · A. C. M. Silva · G. Bannach (✉)
Departamento de Química, Falculdade de Ciências, UNESP, Bauru, SP CEP 17033-260, Brazil
e-mail: gilbert@fc.unesp.br

R. A. E. Castro
CEF, Faculdade de Farmácia, Universidade de Coimbra, CEP 3000-548 Coimbra, Portugal

M. E. S. Eusébio
CQC, Departamento de Química, Universidade de Coimbra, CEP 3004-535 Coimbra, Portugal

O. Treu-Filho
Instituto de Química—UNESP, Araraquara, SP CEP 14800-900, Brazil

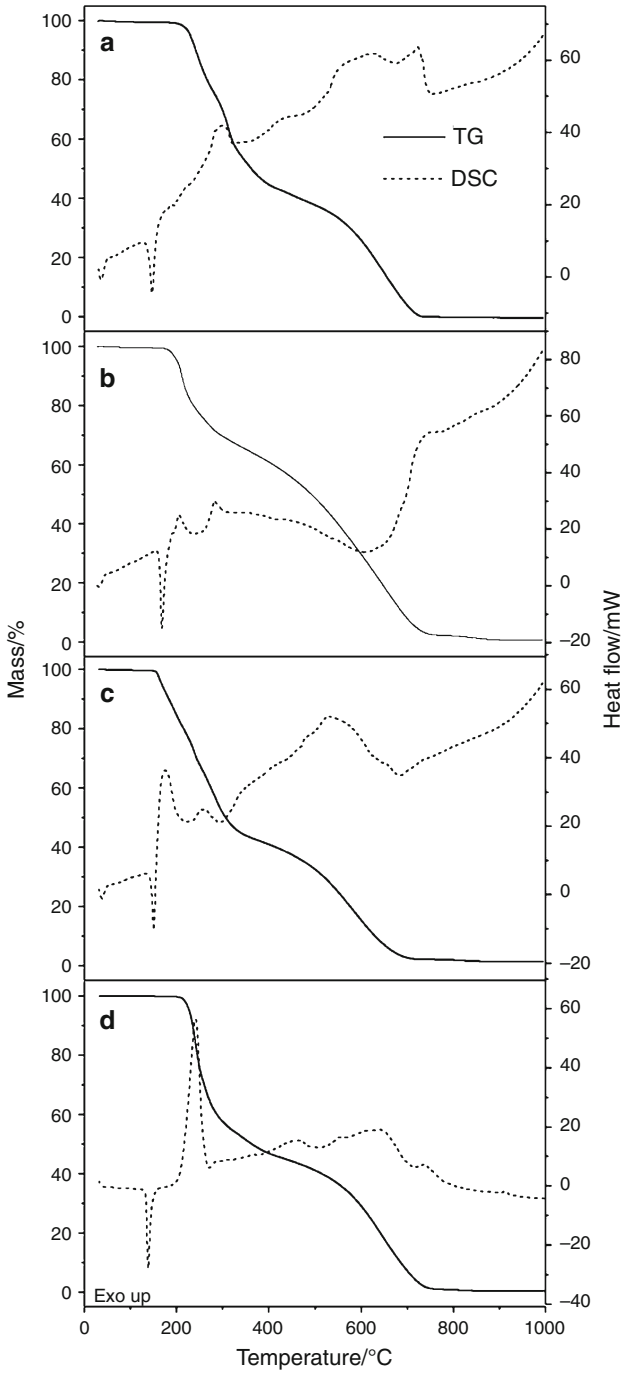

Fig. 1 Simultaneous TG–DSC curves: **a** cimetidine ($m = 5.099$ mg), **b** famotidine ($m = 5.163$ mg), **c** ranitidine-HCl ($m = 5.288$ mg), and **d** nizatidine ($m = 5.093$ mg). Air flow of 50 mL min^{-1} and a heating rate of 20 °C min^{-1}

Theoretical calculations help in interpretations of Fourier transformed infrared (FTIR) spectra supplying structural and physicochemical parameters [14].

Thus, this article aims to the thermal and structural characterization of the following antihistamines: cimetidine, famotidine, ranitidine-HCl, and nizatidine.

Experimental

Samples of cimetidine (batch 20090401 #4) and famotidine (batch FM/005/8035 #2) were purchased from Deg™. Ranitidine-HCl (batch 1003032003) and nizatidine (batch 129K1192) samples were purchased from Galena™ and Fluka®, respectively.

Simultaneous thermogravimetry (TG)–differential scanning calorimetry (DSC) curves were obtained with thermal analysis system, model TGA/DSC 1 Star^e System (Mettler Toledo). The purge gas was an air flow of 50 mL min^{-1}. A heating rate of 20 °C min^{-1} was adopted, with samples weighing about 5 mg. Alumina crucible was used for TG–DSC curves.

DSC curves were obtained with thermal analysis systems model Q-10 (TA Instruments). The purge gas was an air flow of 50 mL min^{-1}. A heating rate of 20 °C min^{-1} was adopted with sample masses between 3 and 5 mg.

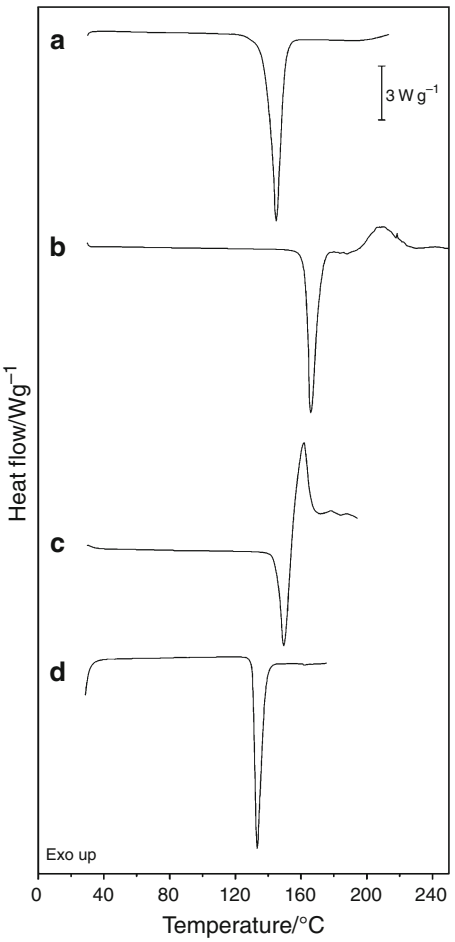

Fig. 2 DSC curves: **a** cimetidine ($m = 3.115$ mg), **b** famotidine ($m = 5.170$ mg), **c** ranitidine-HCl ($m = 5.003$ mg), and **d** nizatidine ($m = 2.945$ mg). Air flow of 50 mL min^{-1} and a heating rate of 20 °C min^{-1}

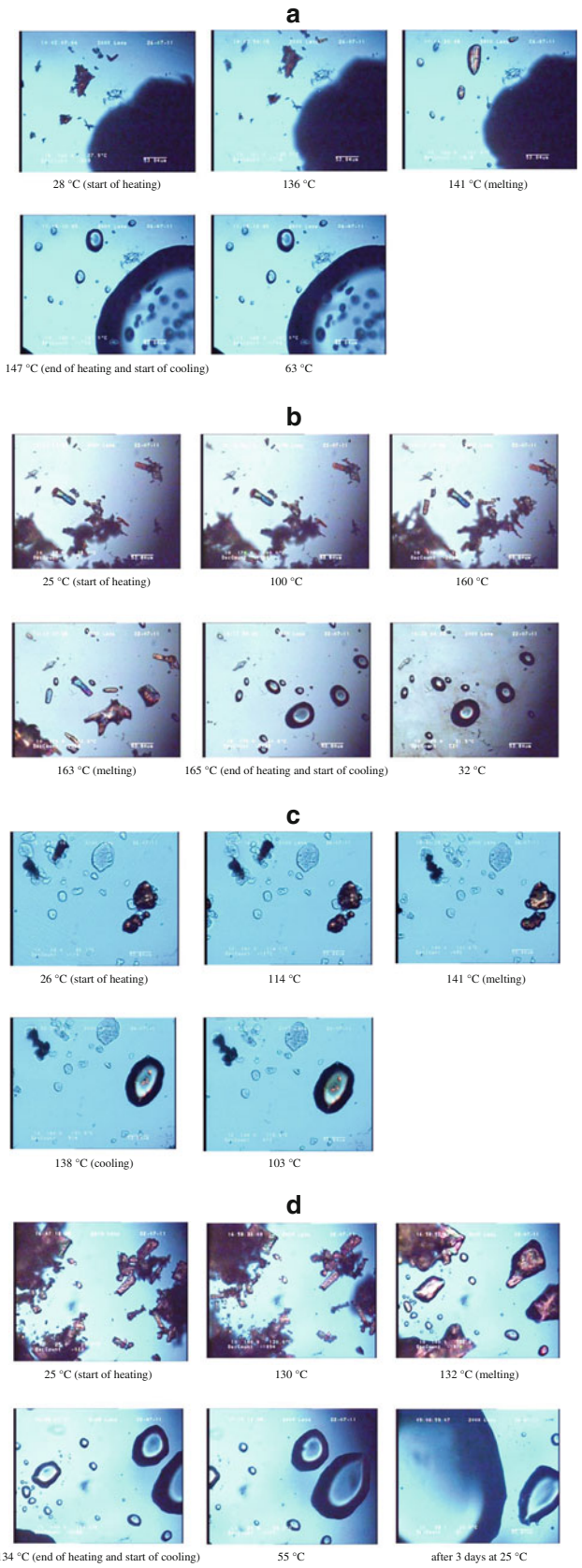

Fig. 3 PLTM images of **a** cimetidine, **b** famotidine, **c** ranitidine-HCl, ▶ and **d** nizatidine. Heating and cooling rates of 10 °C min^{-1} and ×200 magnification

Aluminum crucibles, with perforated cover, were used for recording the DSC curves.

For optical observation, a Leica DMRB microscope, a Sony CCD-IRIS/RGB video camera and Sony HR Triniton monitor were used. Real Time Video Measurement System software by Linkam was used for image analysis. A small amount of the drug was dispersed throughout the sample cell, and covered by a cap. The dispersion aims to study the thermal behavior of individual particles, which is very useful when the drug presents a thermal behavior heterogeneous. The images were obtained by means of combined use of polarized light and wave compensators, giving to the background image a single color and not black.

Infrared spectra were obtained directly by reflectance on a spectrophotometer model FTIR Nicolet iS10 (Thermo Scientific), within the 4,000–600 cm^{-1} range, using an attenuated total reflection (ATR) accessory with a germanium crystal as holder.

The X-ray powder diffraction (XRD) patterns were obtained by means of a Siemens D-5000 X-ray diffractometer, employing Cu Kα radiation ($\lambda = 1.541$ Å) and settings of 40 kV and 20 mA. The sample was placed in the support of the equipment (a glass support) and submitted to radiation ($5° \leq 2\theta \leq 70°$).

In this study, theoretical calculations were used to determine the molecular geometry, infrared spectra of the molecules of the cimetidine, famotidine, ranitidine-HCl, and nizatidine. The quantum chemical approach employed was the three-parameter hybrid theory of Becke [15] using the correlation potential of Lee–Yang–Parr (LYP) [16], and the atomic basis used was the 6-311^{++}g(d) [17, 18] enriched with two diffuse functions and a function of polarization. For the determination of the infrared spectrum was used harmonic field [19] based on the C_1 symmetry (electronic state ^{1}A). The values of frequencies were not scaled, being presented the values of the frequencies, its relative intensities and the description of vibrational modes. The calculations of the vibrational frequencies were also used to determine whether the optimized geometries are a global energy minimum or a saddle point. The Berny algorithm [20] was used for the optimization of the geometries. The molecular calculations were performed using the Gaussian 09 program [21]. The descriptions of the main active vibrational modes were performed with the help of the graphic program GaussView 5.0.8 [22].

Table 1 Comparison of data from theoretical and experimental FTIR

Compound IR data (cm^{-1})	Cimetidine			Famotidine			Ranitidine			Nizatidine		
	ν Theor.	ν Exp.	$\Delta\nu$/%	ν Theor.	ν Exp.	$\Delta\nu$/%	ν Theor.	ν Exp.	$\Delta\nu$/%	ν Theor.	ν Exp.	$\Delta\nu$/%
NH stretch	3596.33	3248.97	10.69	3526.90	3505.27	0.62				3623.54	3279.56	10.49
				3499.26	3399.21	2.94						
				3449.26	3375.46	2.19						
CH stretch in NO_2–CH–										3107.16	3094.22	0.42
C=C conjugated with NO_2										1649.90	1619.67	1.87
Asym. NO_2 stretch conjugated with C–C										1595.33	1585.04	0.65
Thiazole ring										1535.21	1520.99	0.93
CN stretch										1410.80	1420.78	−0.70
CH deformation in NCH_3, CH_2										1480.51	1469.26	0.77
										1456.62	1456.69	0.00
>N–CN stretch	2291.67	2166.01	5.80									
>C–N stretch (ring)	1610.47	1612.93	−0.15									
NO_2 stretch							1523.68	1569.53	−2.921			
CN stretch							1589.04	1620.15	−1.92			
CH stretch				3102.16	3105.02	−0.09						
CH_2 assym. stretch				3060.14	2938.64	4.13						
SO_2 stretch				1276.83	1320.56	−3.31						
CN stretch (thiazole group)				1289.22	1284.34	0.38						

Results and discussion

Thermal analysis

Figure 1a shows that the anhydrous cimetidine displays thermal stability up to 192 °C. It is observed an endothermic peak at 147 °C in the simultaneous TG–DSC curves, which is attributed to the melting of the drug. The drug decomposes in two steps. The first step occurs between 192 and 390 °C, with a mass loss of 54.34%, and it is associated to the exothermic peak at 300 °C. The second step occurs between 390 and 750 °C, with a mass loss of 45.66%, and it is associated to the exotherm between 466 and 750 °C. These thermal events are attributed to decomposition/oxidation of organic matter. The DSC curve (Fig. 2a) shows an endothermic peak at 145 °C (Tonset = 140 °C) attributed to the melting of the drug. The peak temperature observed in this study was consistent with the reports of other authors [23, 24].

Figure 1b shows that the anhydrous famotidine presents thermal stability up to 173 °C. It is observed an endothermic peak at 168 °C (TG–DSC curves) which is attributed to the melting of the drug. The drug decomposes in two steps. The first step occurs between 173 and 400 °C, with a mass loss of 39.10%, and it is associated to the exothermic peaks at 207 and 282 °C. The second step occurs between 400 and 1000 °C with a mass loss of 60.37%, and it is associated to the exotherm between 660 and 900 °C. The residue of 0.53% is attributed to the ash resulting from the thermal decomposition of the drug. These events are attributed to thermal decomposition/oxidation of organic matter. The DSC curve (Fig. 2b) shows an endothermic peak at 166 °C (Tonset = 161 °C) attributed to the melting of the drug. The peak temperature is consistent with the form B of famotidine reported in the literature [25].

Figure 1c shows that the anhydrous ranitidine-HCl displays thermal stability up to 147 °C. It is observed an endothermic peak at 151 °C in the simultaneous TG–DSC curves, which is attributed to the melting of the drug, associated to an exothermic peak at 176 °C, indicating that the drug decomposes itself during melting. The drug

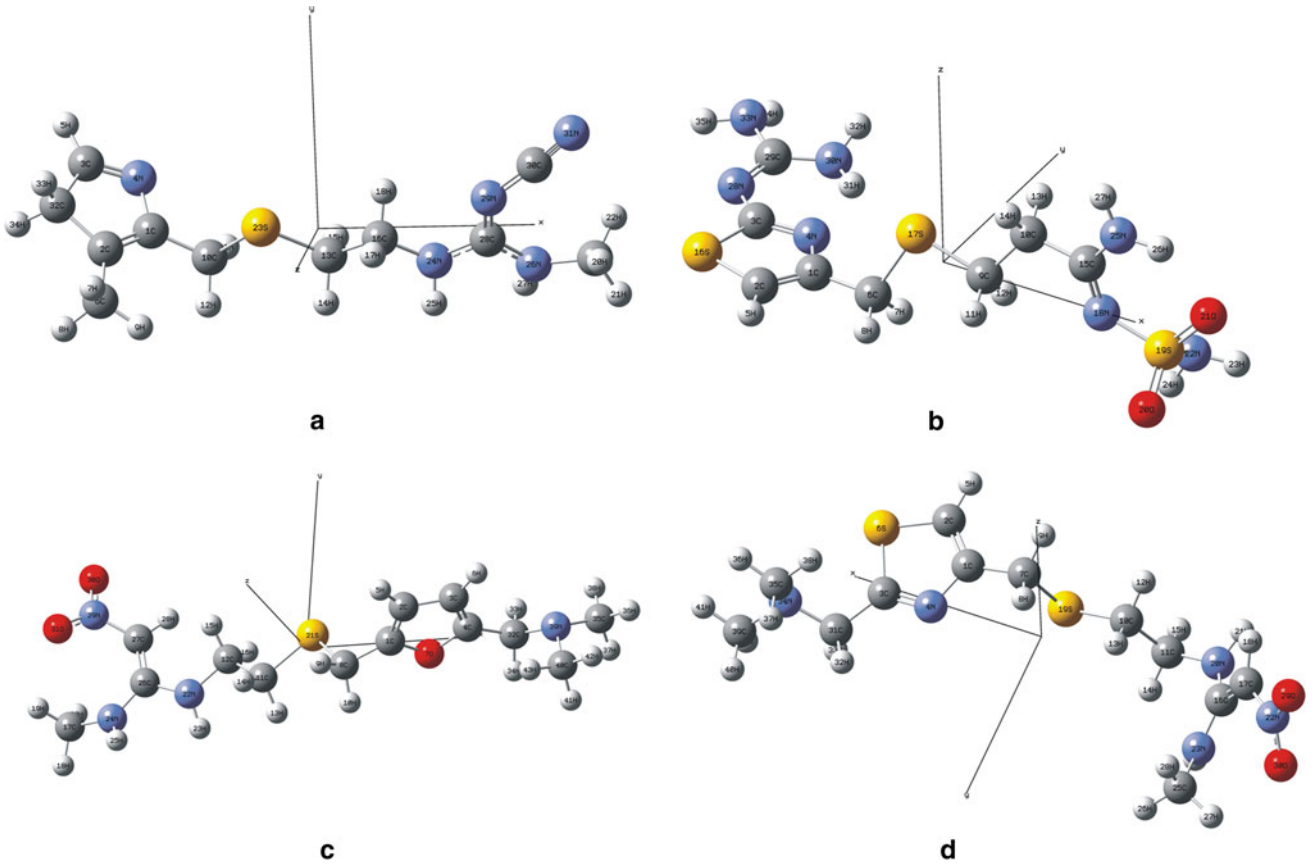

Fig. 4 3D theoretical structures: **a** cimetidine, **b** famotidine, **c** ranitidine-HCl, and **d** nizatidine (optimized using DFT/B3LYP method)

decomposes in two steps. The first step occurs between 147 and 340 °C, with a mass loss of 55.29%, and is associated with the exothermic peaks at 176 and 257 °C in the TG–DSC curves. The second step occurs between 340 and 900 °C with a mass loss of 43.40%, and it is associated to the exothermic peak at 534 °C. The residue of 1.31% is attributed to the ash resulting from the thermal decomposition of the drug. These events are attributed to thermal decomposition/oxidation of organic matter. The DSC curve (Fig. 2c) shows an endothermic peak at 150 °C (Tonset = 144 °C) attributed to the melting of the drug. The peak temperature is in disagreement with those reported found in the literature [26]. These discrepancies may be attributed to the different experimental conditions in the attainment of DSC curves.

Figure 1d shows that the anhydrous nizatidine-HCl displays thermal stability up to 200 °C. It is observed an endothermic peak at 138 °C in the simultaneous TG–DSC curves which is attributed to the melting of the drug. The drug decomposes in two steps. The first step occurs between 200 and 400 °C, with mass loss of 53.16%, and it is associated to the exothermic peak in 242 °C. This large and sharp peak is due to the decomposition of the drug, with the release of NO_2 groups. The release of groups NO_2 was confirmed through qualitative test (the heating of the drug releases a brownish smoke. It confirms the elimination of NO_2 groups). The second step of decomposition occurs between 400 and 900 °C, with a mass loss of 46.54%, and it is associated to the exotherm between 402 and 785 °C in the DSC curve. The residue of 0.3% is attributed to the ash resulting from the thermal decomposition of the drug. These thermal events are attributed to decomposition/oxidation of organic matter. The DSC curve (Fig. 2d) shows an endothermic peak at 133 °C (Tonset = 124 °C) attributed to the melting of the drug.

The simultaneous TG–DSC curves show that the thermal stability of the drugs studied in this study increases in the following order: ranitidine-HCl < famotidine < cimetidine < nizatidine.

Polarized light thermal microscopy (PLTM)

Figure 3 shows that the cimetidine melts itself at 141 °C and evidence neither of crystalline transition during the heating process of the drug, nor of recrystallization during

Table 2 Theoretical data of structure 3D of solid-state anhydrous cimetidine (optimized using DFT/B3LYP method)

Atom no.	Atom symbol	NA	NB	NC	Bond/Å	Angle/°	Dihedral/°	*X*/Å	*Y*/Å	*Z*/Å
1	C							−3.91068	−0.06939	−0.44062
2	C	1			1.35134			−4.87568	−0.29346	0.47845
3	C	1	2		2.18265	78.27583		−5.40561	1.42129	−0.9947
4	N	3	1	2	1.28317	38.89719	179.85875	−4.24765	0.9912	−1.34209
5	H	3	1	2	1.08621	160.57019	−179.06482	−5.89761	2.22939	−1.52834
6	C	2	1	4	1.49371	129.52892	−179.35888	−4.91462	−1.28695	1.59318
7	H	6	2	1	1.09579	111.36357	118.2873	−4.9795	−0.79075	2.56803
8	H	6	2	1	1.09602	111.55405	−122.69656	−5.78857	−1.94392	1.51669
9	H	6	2	1	1.09154	111.90398	−1.69635	−4.02256	−1.91578	1.60955
10	C	1	2	6	1.49119	129.42968	0.18776	−2.59619	−0.7505	−0.61905
11	H	10	1	2	1.09149	109.1662	150.83533	−2.31552	−0.71718	−1.67331
12	H	10	1	2	1.09173	111.57862	30.23154	−2.6361	−1.79183	−0.29363
13	C	10	1	2	2.80158	149.17161	−105.56311	0.19318	−0.70142	−0.36242
14	H	13	10	1	1.09594	84.39374	149.58076	0.09248	−1.7846	−0.2295
15	H	13	10	1	1.09283	87.76042	−101.70551	0.24507	−0.48907	−1.43316
16	C	13	10	1	1.52683	150.32971	26.83166	1.45265	−0.19035	0.33309
17	H	16	13	10	1.09583	110.64722	53.83439	1.39251	−0.35901	1.41419
18	H	16	13	10	1.08901	110.78982	−64.68227	1.56836	0.88218	0.18398
19	C	16	13	10	4.97893	132.85541	−176.71752	6.30876	−0.90927	−0.49824
20	H	19	16	13	1.08907	91.28283	−150.41802	6.53392	−0.78034	0.55947
21	H	19	16	13	1.09082	127.19609	−36.41332	6.79092	−1.82699	−0.83768
22	H	19	16	13	1.09121	110.08902	99.41864	6.72491	−0.06166	−1.04514
23	S	13	10	1	1.8347	40.73764	21.93546	−1.28314	0.12227	0.35041
24	N	16	13	10	1.46265	109.6725	176.56763	2.62965	−0.84761	−0.23437
25	H	24	16	13	1.01014	115.67705	−49.15712	2.57684	−1.85377	−0.30667
26	N	19	16	13	1.45993	22.54724	−2.15663	4.87014	−1.06168	−0.69458
27	H	26	19	16	1.00814	117.06865	178.21917	4.57091	−1.65157	−1.4554
28	C	26	19	16	1.36602	126.05651	8.63452	3.89293	−0.33208	−0.07916
29	N	28	26	19	1.3048	127.72348	12.03259	4.03303	0.76093	0.61956
30	C	29	28	26	1.32049	124.17981	15.63363	5.11752	1.51424	0.60901
31	N	30	29	28	1.16411	173.92323	171.05147	6.00887	2.26093	0.66471
32	C	3	1	2	1.50286	74.27878	0.07471	−5.97532	0.6944	0.1909
33	H	32	3	1	1.09841	111.73662	120.20961	−6.16853	1.3751	1.03103
34	H	32	3	1	1.09829	111.98318	−120.9413	−6.93715	0.21814	−0.04214

Atom no. + NA = bond; atom no. + NA + NB = angle; atom no. + NA + NB + NC = dihedral; *X*, *Y*, *Z* = Cartesian coordinates

its cooling process was observed. These results are in accordance with those found in the literature [24].

According to DSC curves (Fig. 2b, c), the famotidine and ranitidine-HCl decomposes itself during melting and do not suffer any kind of crystalline transition during heating. This thermal behavior can be confirmed by the images obtained through the experiments of thermal microscopy (Fig. 3). The analysis of results shows that the famotidine melts itself at 163 °C, and it neither undergoes any crystalline transition during the heating process nor recrystallizes during the cooling process. At 32 °C, it is possible to verify the presence of brown spots, attributed to the compounds formed during the decomposition of the drug, and which solidifies during the cooling process of the sample. The ranitidine-HCl melts at 141 °C, it neither undergoes crystalline transition during the heating process, nor recrystallizes during the cooling process.

Figure 3 shows that the nizatidine melts at 132 °C and evidence neither of crystalline transition during the heating process of the drug, nor of recrystallization during its

Table 3 Theoretical data of structure 3D of solid-state anhydrous famotidine (optimized using DFT/B3LYP method)

Atom no.	Atom symbol	NA	NB	NC	Bond/Å	Angle/°	Dihedral/°	*X*/Å	*Y*/Å	*Z*/Å
1	C							−2.67143	−1.18803	−0.44966
2	C	1			1.36278			−3.38261	−2.34732	−0.36345
3	C	1	2		2.23571	82.32595		−4.70342	−0.27751	−0.24874
4	N	3	1	2	1.31597	34.86614	−179.86031	−3.41824	−0.03024	−0.38651
5	H	2	1	4	1.07984	128.11045	179.85436	−3.01104	−3.36082	−0.392
6	C	1	2	4	1.4946	125.2279	−179.35464	−1.18899	−1.09639	−0.61638
7	H	6	1	2	1.09265	110.06925	132.7234	−0.94395	−0.38259	−1.40653
8	H	6	1	2	1.09123	110.37132	12.61514	−0.77567	−2.07072	−0.88211
9	C	6	1	2	2.79431	151.63416	−111.00045	1.35862	−0.46388	0.34164
10	C	9	6	1	1.52545	149.82159	5.76998	2.2639	−0.01569	1.4847
11	H	9	6	1	1.09187	86.13499	130.82203	1.65604	−1.45372	−0.01043
12	H	9	6	1	1.08981	86.78774	−120.83948	1.43458	0.22912	−0.49602
13	H	10	9	6	1.09691	109.89832	−60.55807	1.96027	0.97903	1.83336
14	H	10	9	6	1.09532	109.92847	56.15443	2.14777	−0.6906	2.33953
15	C	10	9	6	1.51749	114.26666	178.66539	3.73534	0.06077	1.12167
16	S	2	1	4	1.73694	110.43216	0.10654	−5.07785	−2.00776	−0.19677
17	S	9	6	1	1.83624	40.89912	4.59877	−0.37569	−0.51995	0.9423
18	N	15	10	9	1.30092	117.18607	20.19476	4.03209	0.14597	−0.14208
19	S	18	15	10	1.66019	122.41712	−179.25489	5.59919	0.21831	−0.68539
20	O	19	18	15	1.45745	107.60726	117.80824	5.83241	−0.95618	−1.51626
21	O	19	18	15	1.47387	114.2116	−15.90571	6.58622	0.54772	0.35843
22	N	19	18	15	1.68913	98.8233	−126.2962	5.48517	1.62122	−1.61919
23	H	22	19	18	1.01612	108.4179	163.22998	6.42464	1.96268	−1.80164
24	H	22	19	18	1.01579	110.39376	−75.86504	5.00528	1.42673	−2.49309
25	N	15	10	9	1.34821	115.20299	−160.17799	4.58643	0.03938	2.16707
26	H	25	15	10	1.01314	120.1399	−171.68388	5.57415	0.21252	2.02254
27	H	25	15	10	1.00605	119.90402	−2.25954	4.22673	0.0107	3.10618
28	N	3	1	2	1.35857	164.42689	−179.44231	−5.74585	0.58851	−0.15353
29	C	28	3	1	1.30698	121.33988	−7.39626	−5.55211	1.87731	−0.05522
30	N	29	28	3	1.35907	126.50325	5.89232	−4.36071	2.52498	−0.14556
31	H	30	29	28	1.01716	115.65318	−6.96068	−3.53805	1.92882	−0.19504
32	H	30	29	28	1.00803	118.96245	−156.93174	−4.26599	3.43427	0.2791
33	N	29	28	3	1.37956	117.50646	−173.49373	−6.65615	2.67186	0.17494
34	H	33	29	28	1.00957	117.22401	−146.05824	−6.65942	3.5905	−0.24377
35	H	33	29	28	1.00917	113.24218	−9.86013	−7.52993	2.17473	0.08671

Atom no. + NA = bond; atom no. + NA + NB = angle; atom no. + NA + NB + NC = dihedral; *X*, *Y*, *Z* = Cartesian coordinates

cooling process was observed, even after the sample being kept at 25 °C for 3 days, after cooling.

X-ray diffraction

The XRD patterns (figure not shown) indicates that cimetidine and famotidine are less crystalline compared with ranitidine-HCl and nizatidine.

FTIR with ATR

The FTIR theoretical and experimental data are shown in Table 1. The results indicates that the theoretical bands of FTIR are in agreement to those obtained experimentally, since that in some cases there is no significant difference between the theoretical and experimental values, being even identical in one of the cases. All these bands are in

Table 4 Theoretical data of structure 3D of solid-state anhydrous ranitidine-HCl (optimized using DFT/B3LYP method)

Atom no.	Atom symbol	NA	NB	NC	Bond/Å	Angle/°	Dihedral/°	*X*/Å	*Y*/Å	*Z*/Å
1	C							2.85355	−0.36507	1.0113
2	C	1			1.36192			3.56456	0.2194	2.01513
3	C	2	1		1.43227	106.75841		4.82273	0.61289	1.45515
4	C	3	2	1	1.36098	106.47804	0.01515	4.79537	0.2423	0.14588
5	H	2	1	4	1.08029	125.98482	179.82451	3.23045	0.35622	3.0333
6	H	3	2	1	1.07898	127.81266	−179.80671	5.64421	1.1036	1.95373
7	O	4	3	2	1.36773	109.73849	−0.13249	3.60026	−0.35865	−0.13921
8	C	1	2	3	1.47967	133.44102	−179.05336	1.4989	−0.95531	0.93409
9	H	8	1	2	1.09104	109.69056	−23.68199	1.17749	−1.26928	1.92832
10	H	8	1	2	1.09252	110.42141	−143.60356	1.49913	−1.82497	0.27281
11	C	8	1	2	2.80093	151.44975	104.39973	−1.18935	−0.85139	0.1545
12	C	11	8	1	1.52816	150.39217	−20.29359	−2.41907	−0.05058	−0.27186
13	H	11	8	1	1.09536	88.18212	110.41198	−0.97137	−1.63695	−0.57706
14	H	11	8	1	1.09284	84.29827	−140.90882	−1.37516	−1.32368	1.12234
15	H	12	11	8	1.09079	109.9968	−58.01963	−2.67185	0.68184	0.49592
16	H	12	11	8	1.09784	109.92662	60.0948	−2.20384	0.50205	−1.19572
17	C	12	11	8	4.98778	128.97289	−169.15614	−7.14883	−1.56803	−0.7242
18	H	17	12	11	1.09225	122.06667	−36.26487	−7.40552	−2.5661	−1.08609
19	H	17	12	11	1.09003	115.7208	102.63348	−7.81816	−1.27816	0.08582
20	H	17	12	11	1.09053	89.20447	−147.49387	−7.28105	−0.86164	−1.54445
21	S	11	8	1	1.83464	40.98361	−11.58179	0.26148	0.26492	0.27637
22	N	12	11	8	1.45926	109.78849	−176.74627	−3.55979	−0.94601	−0.43429
23	H	22	12	11	1.0112	115.53572	−49.23583	−3.39003	−1.77121	−0.99354
24	N	17	12	11	1.45459	21.03555	16.98363	−5.75361	−1.57689	−0.313
25	H	24	17	12	1.00875	117.32906	−171.00188	−5.40629	−2.41464	0.12871
26	C	24	17	12	1.35954	126.76101	13.56055	−4.8784	−0.53882	−0.38205
27	C	26	24	17	1.38018	127.06668	21.8477	−5.18539	0.80521	−0.4471
28	H	27	26	24	1.07721	121.41238	−156.8912	−4.49211	1.52024	−0.85755
29	N	27	26	24	1.41157	125.85397	26.74436	−6.35657	1.4111	0.05667
30	O	29	27	26	1.23901	116.73507	−170.99348	−6.54228	2.59912	−0.24211
31	O	29	27	26	1.24173	120.18415	11.26583	−7.12169	0.77149	0.79651
32	C	4	3	2	1.49648	133.81749	177.73311	5.75282	0.39418	−0.99415
33	H	32	4	3	1.096	109.13815	−87.4762	5.57463	1.35662	−1.48726
34	H	32	4	3	1.10615	108.69396	157.28264	5.53045	−0.38246	−1.74977
35	C	32	4	3	2.41316	143.88087	14.8374	8.03651	0.92638	−1.56412
36	H	35	32	4	1.0923	143.65864	23.41552	9.05762	0.94902	−1.17688
37	H	35	32	4	1.10583	95.31333	153.63178	8.04431	0.34793	−2.50656
38	H	35	32	4	1.09236	90.12223	−98.09301	7.74193	1.95232	−1.79631
39	N	35	32	4	1.45653	34.19994	29.31721	7.14538	0.36603	−0.55746
40	C	39	35	32	1.45813	111.36799	126.39951	7.57128	−0.96916	−0.15496
41	H	40	39	35	1.10576	112.52426	−61.17772	7.56868	−1.6863	−0.99663
42	H	40	39	35	1.09233	109.66564	59.201	8.58454	−0.92513	0.25066
43	H	40	39	35	1.09094	110.15919	178.00098	6.91193	−1.35535	0.62367

Atom no. + NA = bond; atom no. + NA + NB = angle; atom no. + NA + NB + NC = dihedral; *X*, *Y*, *Z* = Cartesian coordinates

Table 5 Theoretical data of structure 3D of solid-state anhydrous nizatidine (optimized using DFT/B3LYP method)

Atom no.	Atom symbol	NA	NB	NC	Bond/Å	Angle/°	Dihedral/°	*X*/Å	*Y*/Å	*Z*/Å
1	C							2.33834	−0.97355	0.54502
2	C	1			1.36515			3.25264	−1.98062	0.66135
3	C	1	2		2.21813	81.90188		4.14075	0.16945	−0.05913
4	N	3	1	2	1.29676	35.32173	−179.9287	2.86065	0.2381	0.13634
5	H	2	1	4	1.0803	128.19686	179.03856	3.08635	−3.00089	0.9751
6	S	2	1	4	1.73165	110.6214	0.16928	4.8378	−1.41533	0.25352
7	C	1	2	6	1.49526	125.85422	−179.77772	0.8726	−1.08542	0.8187
8	H	7	1	2	1.09132	109.5054	145.94833	0.50633	−0.14438	1.23256
9	H	7	1	2	1.0912	110.93154	25.43889	0.66849	−1.8907	1.52622
10	C	7	1	2	2.80442	150.2324	−104.98494	−1.76963	−1.26245	−0.10434
11	C	10	7	1	1.53211	150.2455	10.36014	−2.76819	−1.45262	−1.25067
12	H	10	7	1	1.09419	87.602	138.77464	−1.94297	−2.01115	0.67454
13	H	10	7	1	1.09317	85.25686	−112.65215	−1.89498	−0.2711	0.33897
14	H	11	10	7	1.09054	109.74308	−54.13751	−2.56298	−0.73041	−2.0416
15	H	11	10	7	1.09217	110.4828	62.88681	−2.65198	−2.44192	−1.69858
16	C	11	10	7	2.51394	102.32792	−150.4181	−4.75325	−0.12906	−0.45845
17	C	16	11	10	1.38329	133.73884	−49.78279	−5.46644	−0.09127	0.72622
18	H	17	16	11	1.07872	120.77464	−9.40679	−5.29553	−0.8263	1.49703
19	S	10	7	1	1.83556	40.68256	14.43966	−0.05738	−1.4254	−0.74536
20	N	16	11	10	1.38677	29.12826	−116.92564	−4.16648	−1.33135	−0.82358
21	H	20	16	11	1.00979	113.19659	145.55626	−4.51349	−2.1196	−0.29638
22	N	17	16	11	1.41041	126.23282	176.43753	−6.53373	0.77951	1.02934
23	N	16	11	10	1.35248	94.08299	105.32097	−4.53305	0.89571	−1.31317
24	H	23	16	11	1.00821	116.02335	44.84918	−4.31117	0.63979	−2.26279
25	C	23	16	11	1.45502	126.87477	−136.77013	−4.61533	2.31686	−1.01207
26	H	25	23	16	1.09214	108.25131	146.94417	−3.87343	2.83886	−1.62023
27	H	25	23	16	1.08968	112.23143	−91.14051	−5.60955	2.72126	−1.20023
28	H	25	23	16	1.09027	109.44013	28.91661	−4.37616	2.4795	0.03914
29	O	22	17	16	1.23948	116.76637	−173.68886	−6.97041	0.7448	2.18882
30	O	22	17	16	1.24178	120.133	8.39	−7.01709	1.50469	0.14475
31	C	3	1	2	1.50393	159.88624	172.07985	4.98968	1.29829	−0.57571
32	H	31	3	1	1.10309	107.7239	26.79533	4.44646	2.23991	−0.38842
33	H	31	3	1	1.09527	108.19765	−88.11848	5.0717	1.19475	−1.66299
34	N	31	3	1	1.45796	112.56745	152.53062	6.33648	1.28634	−0.01748
35	C	34	31	3	1.45944	112.20543	−74.29487	6.36197	1.73467	1.37116
36	H	35	34	31	1.09199	109.66203	173.95408	7.36674	1.60822	1.7797
37	H	35	34	31	1.10458	112.47904	−65.48761	6.07566	2.79618	1.47757
38	H	35	34	31	1.0914	110.28615	55.22799	5.67631	1.13705	1.97439
39	C	34	31	3	1.45731	112.2277	159.24669	7.27987	2.03536	−0.83768
40	H	39	34	31	1.10483	113.07452	63.88482	7.04258	3.11283	−0.89601
41	H	39	34	31	1.09216	109.48561	−175.79571	8.28443	1.93524	−0.42097
42	H	39	34	31	1.09222	110.0436	−57.32527	7.29527	1.63267	−1.85283

Atom no. + NA = bond; atom no. + NA + NB = angle; atom no. + NA + NB + NC = dihedral; *X*, *Y*, *Z* = Cartesian coordinates

agreement to those found in the literature [2–4, 25, 27] and the theoretical structures for each drug are shown in Fig. 4, with its theoretical data depicted in Tables 2, 3, 4, 5.

Conclusions

The TG–DSC curves provided information on the thermal stability of the compounds studied, which increases in the

following order: ranitidine-HCl < famotidine < cimetidine < nizatidine.

The thermomicroscopy experiments confirmed the information obtained from the analysis of TG–DSC and DSC curves, in relation to thermal stability and thermal decomposition of the compounds studied. These experiments also revealed information about the irreversibility of thermal processes that occurs during heating and cooling of the antihistamines studied.

The XRD patterns allowed observing that cimetidine and famotidine are less crystalline compared with ranitidine-HCl and nizatidine.

The quantum calculations performed allowed the comparison between the theoretical and experimental absorption bands, for each of the four drugs studied, since in some cases, virtually no differences between the theoretical and experimental values, being even identical in one of the cases. All absorption bands are very close to those found in the literature.

Acknowledgements The authors thank FUNDUNESP, PROPe-UNESP, PROPG-UNESP, FC-UNESP, and POSMAT-UNESP for the financial support. The authors also thank Prof. Dr. Massao Ionashiro by the use their equipment, TG–DTA, DSC, FTIR and the Center for Scientific Computing (NCC/GridUNESP) of Universidade Estadual Paulista (UNESP), Instituto de Quimica de Araraquara, UNESP Campus de Araraquara and CENAPAD—UNICAMP.

References

1. Hoyte FCL, Katial RK. Antihistamine therapy in allergic rhinitis. Immunol Allergy Clin N Am. 2011;31:509–43.
2. Bavin PMG, et al. Cimetidine. In: Florey K, editor. Analytical profiles of drug substances. New York: Academic Press; 1984. p. 128–81.
3. Hohnjec M, et al. Ranitidine. In: Florey K, editor. Analytical profiles of drug substances. New York: Academic Press; 1984. p. 533–61.
4. Wozniak TJ. Nizatidine. In: Florey K, editor. Analytical profiles of drug substances. New York: Academic Press; 1984. p. 397–424.
5. The Merck Index, Merck & Co. Inc., 11th ed. New York: Rohway; 1989.
6. Schmidt AC, Senfter N, Ferroni DC, Griesser UJ. Crystal polymorphism of local anaesthetic drugs. J Therm Anal Calorim. 2003;73:397–408.
7. Plano D, Lizarraga E, Palop JA, Sanmartín C. Study of polymorphism of organosulfur and organoselenium compounds. J Therm Anal Calorim. 2011;105:1007–13.
8. Giordano F, Novak C, Moyano JR. Thermal analysis of cyclodextrins and their inclusion compounds. Thermochim Acta. 2001;380:123–51.
9. Neto HS, Novak C, Matos JR. Thermal analysis and compatibility studies of prednicarbate with excipients used in semi solid pharmaceutical form. J Therm Anal Calorim. 2009;97:367–74.
10. Bernardi LS, Oliveira PR, Murakami FS, Silva MAS, Borgmann SHM, Cardoso SG. Characterization of venlafaxine hydrochloride and compatibility studies with pharmaceutical excipients. J Therm Anal Calorim. 2009;97:729–33.
11. Petit S, Mallet F, Petit MN, Coquerel G. Role of structural and macrocrystalline factors in the desolvation behaviour of cortisone acetate solvates. J Therm Anal Calorim. 2007;90:39–47.
12. Wesolowski M, Szynkaruk P. Thermal decomposition of purine derivatives used in medicine. J Therm Anal Calorim. 2001;65:599–605.
13. Schnitzler E, Kobelnik M, Sotelo GFC, Bannach G, Ionashiro M. Thermoanalytical study of purine derivatives compounds. Ecl Quim. 2004;29:71–8.
14. Bannach G, Arcaro R, Ferroni DC, Siqueira AB, Treu-Filho O, Ionashiro M, Schnitzler E. Thermal analytical study of some anti-inflammatory analgesic agents. J Therm Anal Calorim. 2010;102:163–70.
15. Becke AD. Density-functional thermochemistry. 3. The role of exact exchange. J Chem Phys. 1993;98:5648–52.
16. Lee C, Yang W, Parr RG. Development of the Colle–Salvetti correlation-energy formula into a functional of the electron density. Phys Rev B. 1988;37:785–9.
17. Petersson GA, et al. A complete basis set model chemistry. I. The total energies of closed-shell atoms and hydrides of the first-row atoms. J Chem Phys. 1988;89:2193–218.
18. Petersson GA, Al-Laham MA. A complete basis set model chemistry. II. Open-shell systems and the total energies of the first-row atoms. J Chem Phys. 1991;94:6081–90.
19. Goodson DZ, Sarpal SK, Wolfsberg M. Influence on isotope effect calculations of the method of obtaining force constants from vibrational data. J Phys Chem. 1982;86:659–63.
20. Li X, Frisch MJ. Energy-represented DIIS within a hybrid geometry optimization method. J Chem Theory Comput. 2006;2:835–9.
21. Frisch, MJ et al. Gaussian 09, Revision A.02.Wallingford: Gaussian, Inc.; 2009.
22. Dennington R, Keith T, Millam J. GaussView, Version 5.0.8, Semichem Inc., Shawnee Mission KS; 2000–2008.
23. Sanders GHW, et al. Discrimination of polymorphic forms of a drug product by localized thermal analysis. J Microsc. 2000;198:77–81.
24. Souza FS, Macedo RO, Veras JWE. Studies of cimetidine preformulated and tablets for TG and DSC coupled to the photovisual system. Thermochim Acta. 2002;392–3:99–106.
25. Lin SY, Cheng WT, Wang SL. Thermodynamic and kinetic characterization of polymorphic transformation of famotidine during grinding. Int J Pharm. 2006;318:86–91.
26. Mirmehrabi M, et al. Characterization of tautomeric forms of ranitidine hydrochloride: thermal analysis, solid-state NMR, X-ray. J Cryst Growth. 2004;260:517–26.
27. Al-Omar MA, Al-Mohizea AM. Famotidine. In: Brittain HG, editor. Profiles of drug substances, excipients and related methodology. Amsterdan: Elsevier; 2009. p. 115–51.